Optical and Quantum Electronics (2022) 54:775
https://doi.org/10.1007/s11082-022-04199-1

Investigation of high-speed hybrid WDM-OCDMA-PON system incorporating integrated fiber-FSO link under distinct climate conditions

Meet Kumari[1] · **Vivek Arya**[2]

Received: 29 July 2022 / Accepted: 10 September 2022 / Published online: 29 September 2022

Abstract
In this paper, a high-speed hybrid wavelength division multiplexing optical code division multiple access passive optical network (WDM-OCDMA PON) to offer information to the integrated fiber-free space optics (FSO) link of 60 km fiber and 500 m FSO length for 100 users under the impact of different weather conditions has been presented and investigated. The mathematical analysis and simulation results reveal that a hybrid 10 km of fiber and 500 m of FSO range using a modified new zero-cross correlation (MNZCC) code under the influence of different climate conditions for 64 users can be achieved. The hybrid FSO and fiber length of 10 m and 60 km respectively, at received power of 4dBm and signal-to-noise ratio (SNR) of 34 dB are also achieved under the impact of fiber impairments and atmospheric turbulence. Moreover, the performance comparison of the proposed system with the previous recent work in literature discloses its dominance over others in terms of code selection.

Keywords Passive optical network (PON) · Optical code division multiple access (OCDMA) · Wavelength division multiplexing (WDM) · Free space optics (FSO) · Modified new zero-cross correlation (MNZCC)

1 Introduction

At present, greater than 70 million individuals pay an extra to access data-rich applications utilizing primarily high-speed links like digital subscriber line (DSL), co-axial cable, optical fiber, 4G/5G cellular, and satellite. Millions more want to connect them but are incapable to do so, because of two key reasons i.e. cost and bandwidth demerits. The service providers experience restrictions as they attempt to provide high-speed access to excitedly

✉ Meet Kumari
meetkumari08@yahoo.in

Vivek Arya
ichvivekmalik@gmail.com

[1] Department of ECE, Chandigarh University, Mohali, India

[2] Department of ECE, FET, Gurukula Kangri (Deemed to be University), Haridwar, India

awaiting users. This is due to the deficit of infrastructure, cost competition, regulatory issues and last mile challenges. Free space optics (FSO) technology can subdue all these issues considerably reducing the cost and deployment time. Interception and interference free transmissions make FSO, an optical wireless communication the most favoured wireless technology. It is line of sight (LOS) communication that offers high data rate (Gbps), utilizing huge optical bandwidth in a cost effective way. Video surveillance along with monitoring, short range connectivity, disaster recovery, back-haul system, security and broadcasting are its applications. In spite of having various merits, FSO has certain disadvantages like the wave propagation is hugely affected by scintillation, turbulence, scattering and molecular absorption. Heavy snow and fog too have a harsh impact on FSO links. Several studied had been completed by different researchers to improve the transmission rate of these links and also proposed various techniques to handle the different atmospheric turbulences (Anuranjana et al. 2022; Kakati and Arya 2019; Mandal et al. 2018).

Further, in the past few years, hybrid passive optical network (PON) and FSO offer a series of significant broadband access technologies that provide several advantages like high quality services, high data rate wired/wireless access and various other cost-effective services. In addition, as resource configuring is a significant feature of any network with expected growth, in particular, the access segments of forthcoming networking configurations PON/FSO. In order to sustain the expected growth in customer density, PON/FSO should embrace scalable layouts, which would permit them to effortlessly support a raised number a full-duplex transmission. The capacity of hybrid PON/FSO systems may be enhanced by using different multiplexing techniques. To scale-up these systems, wavelength division multiplexing (WDM) based PON helps in utilizing the full-capability of FSO systems (Ratnam et al. 2009). Also, the single ray FSO systems are susceptible to varying climate conditions, so multi-ray systems may be combined by employing WDM technique for an improved performance and reducing the turbulent effects (Anuranjana et al. 2022; Naqshbandi and Jha 2016; Xu et al. 2021). Recently, Anuranjana et al. proposed a mode division multiplexing (MDM)-WDM FSO system using dual polarization-quadrature phase shift keying (DP-QPSK) modulation at 1Tbps over 20 km clear weather condition (Anuranjana et al. 2022). Chaudhary et al. illustrated the MDM-WDM using orthogonal frequency division multiplexing radio-over-free-space-optics (OFDM Ro-FSO) at 120 Gbps (Chaudhary et al. 2018). The results show that using donut modes (DT) in the system offers 80 km acceptable transmission distance. Li CY et al., proposed and demonstrated a WDM four level pulse amplitude modulation (4PAM) FSO system and under water communication (UWC) at 100Gbps data rate over 500 m FSO and 5 m in FSO and clean undersea links respectively (Li et al. 2020). In (Singh et al. 2021), a high speed 16×10Gbps WDM-FSO system employing OFDM modulation over the FSO link of 10.75 km is proposed. A WDM-FSO system for 51 km transmission distance at 40Gbps is investigated (Yeh et al. 2020a). Ciaramella E et al., successfully implemented a 40Gbps WDM-FSO system over 210 m FSO link for 32 users (Ciaramella et al. 2009). Dayal et al., proposed a 2.5 Gbps WDM FSO system under different weather conditions. The results shows that under light rain a successful 27 km transmission distance can be achieved (Dayal et al. 2017).

Simultaneously, optical code division multiple access (OCDMA) is widely utilized in wireless technologies as it provides attractive pros like security, spectral efficiency, asynchronous data transmission, soft capacity-on-demand etc. (Al-Khafaji et al. 2012). These advantages make OCDMA an engaging technology for next generation PON (NG-PON) based networks. Taking into account the benefits of both hybrid WDM-FSO PON and OCDMA, their integration has enticed researcher, especially tolerance to the

environment degrading factor of FSO (Cao and Gan 2012; Moghaddasi et al. 2015; Mukherjee et al. 2020a) This work had been proposed in (Kumar and Singh 2014), where an OCDMA-FSO system upto 8 km at 2.5 Gbps transmission rate is presented. In (Ratnam et al. 2009), a hybrid WDM-OCDMA PON at 2.4 Gbps over 20 km is successfully examined. In (Cao and Gan 2012), a hybrid WDM-OCDMA PON at both downstream and upstream data rate of 2.5 Gbps over 22 km is successfully proposed. Ji et al., designed and demonstrated a 10Gbps FSO-OCDMA system over 1.8 m wireless range (Ji et al. 2020). In (Moghaddasi et al. 2015), a FSO system based on spectral amplitude coding (SAC)-OCDMA over 2.6 km for ten users has been proposed and designed. In these proposed systems, researchers generally focus attention on hybrid or non-hybrid WDM-OCDMA PON with FSO channel but don't look out to OCDMA codes. Also, the complete scheme of network design based on hybrid WDM-OCDMA-FSO PON for different FSO losses, atmospheric conditions and turbulence are rarely investigated (Cao and Gan 2012; Dutta et al. 2022; Jiao et al. 2019).

The motivation behind the proposed system is to select and advances the 5G technology that handles the wide bandwidth applications and services to best tackle the subscribers' needs. Although, the recent FSO wireless systems are becoming more advantages for using in fiber-to-the-x (FTTx), hospitals, manufacturing, business and industrial automation applications. But FSO based systems can't be regarded as a full replacement for various traditional wired systems such as time division multiplexing PON (TDM-PON) and WDM-PON, OCDMA-PON, at a minimum in the mid-way. This is because of wireless systems corns like low throughput per-node, presence of unpredictable communication delays, unwanted congestion and diverse environment conditions. This shortcoming can be overcome by utilizing hybrid fiber-FSO links more preferably in existing energy efficient and next generation PONs. Hence, in this paper a hybrid WDM-FSO-OCDMA PON employing different OCDMA codes with integrated fiber-FSO link is demonstrated to attain the improved capacity, flexibility and efficiency (Alsharif et al. 2018; Cena et al. 2008; Dutta et al. 2021). Also, this system can enhance the network resource utilization, unlock the network potential and forward towards achieving promising research results for the future communication as well as networking demands in different scenario. Moreover, this hybrid bidirectional system reduces multi-access interference (MAI) and phase-induced intensity noise (PIIN), Rayleigh backscattering (RB) noise, and inter-channel interference (ISI) effectively as compared to other conventional PONs (Yeh et al. 2019). The main contributions of this work are as follows:

- To propose and design the hybrid WDM-FSO-OCDMA PON system employing different OCDMA codes under the impact of different weather conditions viz. clear air, haze, rain and dust-fog as well as FSO channel losses.
- To compare its performance in terms of different codes viz. modified new zero-cross correlation (MNZCC), multi-diagonal (MD), hadamard, shift zero cross-correlation (ZCC), ZCC, flexible cross correlation (FCC) and modified quadratic congruence (MQC) by considering fiber nonlinearities, attenuation, dispersion and noise.
- To compare the performance of the proposed system with the previous recent work in literature.

The rest of the paper is organized as—Sect. 2 explains the mathematical analysis of the system performance. Block architecture and simulated design is presented in Sect. 3 followed by results and analysis in Sect. 4. Finally, conclusion is elucidated in Sect. 5.

2 Mathematical analysis of the system performance

To analyse the performance of the hybrid WDM-FSO-OCDMA PON using distinct codes, signal to noise ratio (SNR) and bit error rate (BER) of system are determined using Gaussian approximation under the impact of PIIN (ρ_{PIIN}), thermal noise ($\rho_{thermal}$), shot noise (ρ_{shot}). The four primary assumptions are considered to analyse the performance of proposed system as below (Anuar et al. 2009):

- All light sources are un-polarised.
- All light sources consist of flat spectrum over the bandwidth $\left[f_0 - \frac{B}{2}, f_0 + \frac{B}{2}\right]$, where f_0 and B is central frequency and source bandwidth respectively.
- All the spectral components have comparable spectral width.
- Alike power is attained at the receiver side.
- Synchronized all bits from each subscriber.

At receiver side, photo detector variance, is given as (Bhanja and Panda 2017; Nisar et al. 2019):

$$\rho^2 = \rho_{shot} + \rho_{thermal} + \rho_{PIIN} \tag{1}$$

where,

$$\rho_{shot} = 2eBi \tag{2}$$

$$\rho_{thermal} = \frac{4KBT}{R} \tag{3}$$

$$\rho_{PIIN} = i_{PIIN}^2 Bt \tag{4}$$

where e, B, i, K, R, T, t and i_{PIIN} are electron charge, electric bandwidth, photocurrent, Boltzmann constant, receiver load, receiver noise temperature, source coherent time and photo noise current respectively. Let P_k and P_l are two distinct sequences of code. So, MNZCC code's correlation properties with direct detection design can be given as (Anuar et al. 2009; Hussein et al. 2011; Panda 2017):

$$\sum_{j=1}^{s} P_k(j)P_l(j) = \left\{ \begin{array}{l} w, \ Fork = l \\ 0, \ Else \end{array} \right\} \tag{5}$$

where s, w and l are number of subscribers, code weight and code length respectively. Further at receiver, the optical source coherent time, t, can be given in terms of single sideband (SSB) power spectral density (PSD) of photodiode (PD) incidence light $H(f)$ as below (Anuar et al. 2009):

$$t = \frac{\int_0^\infty H(f)^2 df}{\left[\int_0^\infty H(f) df\right]^2} \tag{6}$$

In addition, to measure the SNR, PD current (i) is calculated as follows (Hussein et al. 2011):

$$i = R \int_0^{\infty} H(f)df \tag{7}$$

where R presents PD responsivity. Further, the PSD for hybrid PON using MNZCC code is expressed as (Anuar et al. 2009):

$$\int_0^{\infty} H(f)df = \frac{P_r}{l}[(s-1+w)w] \tag{8}$$

where P_r means the received power. Hence, the PD current, i can be given as (Anuar et al. 2009):

$$i = R\frac{P_r}{l}[(s-1+w)w] \tag{9}$$

and the SNR can be measured as (Bhanja and Panda 2017; Nisar et al. 2019):

$$SNR = \frac{i^2}{i^2_{totalnoise}} \tag{10}$$

where,

$$i^2_{totalnoise} = i^2_{shot} + i^2_{thermal} + i^2_{PIIN} \tag{11}$$

At receiver side, the total noise current, $i^2_{totalnoise}$, with disregarding PIIN noise due to the zero cross-correlation property of MNZCC code with probability of 0.5 of transmission bit '1' can be written as (Anuar et al. 2009):

$$i^2_{totalnoise} = eRB\frac{P_r}{l}[(s-1+w)w] + \frac{4KBT}{R} \tag{12}$$

Using Eqs. (9), (10) and (12) the SNR for the proposed work using MNZCC, ZCC, MD, MQC, shift ZCC, hadamard, FCC codes can be measured as follow (Anuar et al. 2009):

$$SNR_{MNZCC} = \frac{2\left[\frac{RwP_r}{l}\right]^2}{\left[\frac{P_r eBR}{l}\right](s-1+w)w + \frac{4BKT}{R}} \tag{13}$$

$$SNR_{ZCC} = \frac{2\left[\frac{RwP_r}{l}\right]^2}{\left[\frac{P_r eBR}{N}\right](s-1+w)w + \frac{4BKT}{R}} \tag{14}$$

$$SNR_{MD} = \frac{\left[\frac{Rw^2P_r}{l}\right]^2}{\left[\frac{w^2eBRP_r}{l}\right] + \left[\frac{4BKT}{R}\right]} \tag{15}$$

$$SNR_{MQC} = \frac{\left[\frac{RP_r}{p}\right]^2}{\frac{BP_r^2R^2s\left(\frac{s-1}{p}+p+s\right)}{[2\Delta B(p+1)p^2]} + \frac{eBRP_r(p-1+2s)}{[p^2+p]} + \frac{4BTK}{R}} \tag{16}$$

$$SNR_{ShiftZCC} = \frac{\left[\frac{Rw^2P_r}{N}\right]^2}{\left[\frac{w^2eBRP_r}{l}\right][w+3] + \left[\frac{BR^2P_rw}{2\Delta B}\right] + \left[\frac{2BKT}{R}\right]} \tag{17}$$

$$SNR_{Hadamard} = \frac{4\Delta f}{B(2^c-1)^2} \tag{18}$$

$$SNR_{FCC} = \frac{\left[\frac{RwP_r}{l}\right]^2}{\left[\frac{2eBRP_r}{w}\right][w+3] + BR^2\left[\frac{P_r^2sw}{\Delta Bl^2}\right][s+3] + \frac{4BKT}{R}} \tag{19}$$

where p and c present prime number and code's cardinality ≥ 2 respectively. Ultimately, to evaluate the BER, Gaussian approximation is considered and the obtained BER is given as below (Anuar et al. 2009):

$$BER = \frac{1}{2}erfc\sqrt{\frac{SNR}{8}} \tag{20}$$

where *erfc* implies the error function. Again, the FSO link under distinct atmospheric climate conditions can be given as (Amphawan et al. 2019; Fazea 2019):

$$P_r = P_t.\left(\frac{a_r}{(\theta z)^2}\right)\cdot exp(-\beta z) \tag{21}$$

where $P_{t,,}$ a_r, z, θ and β are the transmitted power, effective receiver antenna aperture area, transmission distance, beam divergence and haze, fog or rain dependence appearance factor respectively. In this work, Gamma Gamma (GG) fading distribution model is chosen for different attenuation over a wide range of atmospheric turbulence as below (Yeh et al. 2020b; Yousif et al. 2019):

$$f_x(x) = \frac{2(qt)^{\left(\frac{q+t}{2}\right)}}{\Gamma(q)\Gamma(t)}.x^{\left(\frac{q+t}{2}\right)-1}J_{q-t}\left[2(qtx)^{\frac{1}{2}}\right] \tag{22}$$

where x, J_{q-t} and $\Gamma(.)$ are atmospheric turbulence, modified Bessel function along with its order $(q-t)$ and Gamma function respectively. The number of wide scale effective eddies, (q) and small scale effective eddies (t) are given as (Huszaník et al. 2018; Yeh et al. 2020b; Yousif et al. 2019):

$$q = \frac{1}{\left[exp\left\{\frac{0.49k_0^2}{\left(1+0.18d^2+0.56k_0^{\frac{12}{5}}\right)^{\frac{7}{6}}}\right\}-1\right]} \tag{23}$$

and

$$t = \frac{1}{\left[exp\left\{\frac{0.51k_0^2\left(1+0.18d^2+0.56k_0^{\frac{12}{5}}\right)^{\frac{-5}{6}}}{\left(1+0.90d^2+0.62d^2k_0^{\frac{12}{5}}\right)^{\frac{5}{6}}}\right\}-1\right]} \tag{24}$$

where $d = \sqrt{\frac{kD_r^2}{4z}}$ represents the diameter of the spherical wave with D_r denotes the receiver aperture diameter, k_0 is the aperture-average. Table 1 shows the basic properties of various OCDMA codes for comparative performance analysis of the system.

3 System description

Figure 1 illustrates the proposed NG-PON based hybrid WDM-OCDMA-PON at transmission rate of 10/2.5 Gbps downlink/uplink per channel using integrated fiber-FSO link.

For hybrid WDM-OCDMA PON, seven one dimensional OCDMA codes viz. MNZCC, hadamard, MD, shift ZCC, FCC, ZCC and MQC codes are utilized to evaluate the proposed system performance over fiber-FSO link for varying FSO range, fiber length, received power and distinct number of users. Here, the hybrid WDM-OCDMA

Table 1 Comparison of various OCDMA codes (Bhanja and Panda 2017; Hussein et al. 2011; Nisar et al. 2019; Panda 2017; Rashidi et al. 2010; Rashidi[a] et al. 2013; Samanta et al. 2019; Wei et al. 2001)

Code	Number of subscribers (s)	Cross correlation (λ_{cross})	Length of the code (l)	Weight of the code (w)	Code design for two subscribers
MNZCC	s	0	$w^2 + 2w$	w	$\begin{bmatrix} 0 & 0 & 1 \\ 0 & 1 & 0 \\ 1 & 0 & 0 \end{bmatrix}$
Hadamard	$2^c - 1$	2^{c-2}	2^c	2^{c-1}	$\begin{bmatrix} 1 & 1 \\ 1 & 0 \end{bmatrix}$
MD	s	0	ws	w	$\begin{bmatrix} 1 & 0 & 0 & 1 \\ 0 & 1 & 1 & 0 \end{bmatrix}$
ZCC	$w + 1$	0	$w(w + 1)$	w	$\begin{bmatrix} 1 & 0 \\ 0 & 1 \end{bmatrix}$
Shift ZCC	$w + 1$	0	ws	w	$\begin{bmatrix} 1 & 0 \\ 0 & 1 \end{bmatrix}$
FCC	s	≤ 1	$ws - \lambda_{max}$ $(s - 1)$	w	$\begin{bmatrix} 1 & 1 & 0 \\ 0 & 1 & 1 \end{bmatrix}$
MQC	s	1	$p^2 + p$	$p + 1$	Not for 2

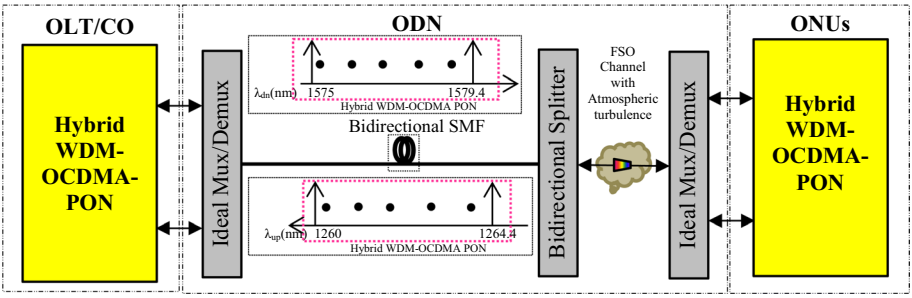

Fig. 1 Conceptual diagram of bidirectional hybrid WDM-OCDMA PON using integrated fiber-FSO link

PON employing distinct codes consists of maximum 12 wavelengths both for downlink (1575–1579.2 nm) and uplink (1260–1264.4 nm) transmission with 0.4 nm channel spacing at 120 Gbps (12 × 10 Gbps) and 30 Gbps (12 × 2.5 Gbps) data rate respectively (Curri et al. 2014; Effenberger and Lin 2009; Mukherjee et al. 2020b).

Also, the integrated fiber-FSO optical access communication is used to achieve the long reach transmission with high capacity and reliability under clear air, haze, rain and dust fog weather conditions. The hybrid WDM-OCDMA-FSO PON can provide wired/wireless access with high reliability and high capacity backhaul support to accomplish the long-reach transmission needs for different services like residential, business and backhaul networks etc. To realize the proposed system under the impact of different environment conditions, major constraints related to FSO link are considered. Figure 2 illustrates the block diagram of the proposed bidirectional hybrid WDM-OCDMA PON with fiber-FSO links.

At optical line terminal (OLT) side, for downstream hybrid WDM-OCDMA PON architecture employing MNZCC code $x \times y$ (x = number of codes and y = number of available wavelengths), ONUs are sub-divided into x groups, where y users with distinct wavelengths in single group share the same OCDMA code as shown in Fig. 2a. The different wavelengths (1575–1579.2 nm having 0.4 nm spectral width) continuous wave (CW) laser sources at input power (P_{in}) of 10 dBm are used to originate four optical signals. These signals are modulated with 10 Gbps NRZ pseudo random bit sequence (NRZ-PRBS) at an aggregate bit rate of 120 Gbps (12 × 10 Gbps) using Mach–Zehnder Modulator (MZM). For the proposed code, y CW laser diodes are utilized by $x \times y$ ONUs to overcome the cost of system. For this, y wavelengths are multiplexed by array waveguide grading (AWG) multiplexer followed by a power splitter which splits the coded signals into x parts, and then fed into the corresponding AWG*1* to AWG*x*. Further these multi-wavelength coded channels combined by $y \times 1$ AWG*1*. The downstream WDM-OCDMA-PON transmitter section using MNZCC code is shown in Fig. 2b Also, the encoder design of different code design is presented in Fig. 2c. Then the signals are passed to single $x \times 1$ Ideal Mux, optical circulator and bidirectional single mode fiber (SMF). At the ONU side of WDM-OCDMA PON, all the incoming downward signals form central office (CO) is split into x parts by a 1×2 bidirectional power splitter followed by a FSO cannel and then x groups of signals are broadcast to each OCDMA channel for decoding. After decoding, the multi-wavelength signals are demultiplexed by AWG at the corresponding optical network unit (ONU) followed by a receiver section which is used to detect and analysed the performance of system in downstream direction. Here, the receiver section consists of PIN photodetector, low pass Bessel filter and 3R regenerator to convert incoming optical signal to electrical signal, select the

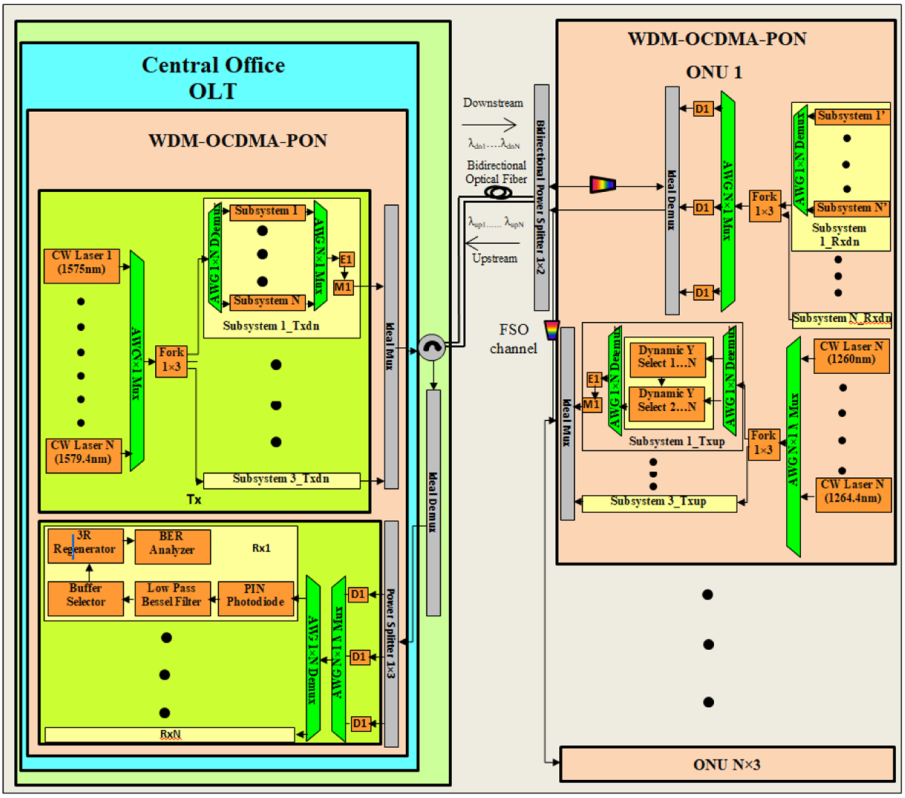

(a)

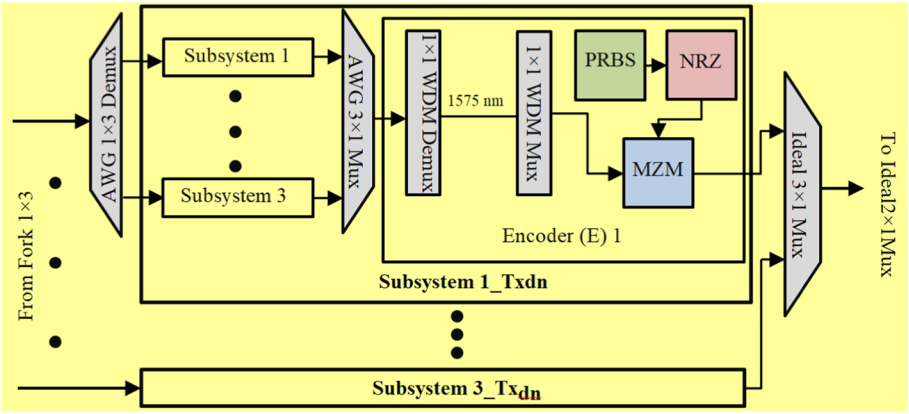

(b)

Fig. 2 **a** Architecture of full-duplex hybrid WDM-FSO-OCDMA PON using various codes, **b** downstream WDM-OCDMA-PON transmitter section for MNZCC code, different code design for **c** encoder and **d** decode; uplink **e** time switch section and **f** transmitter section

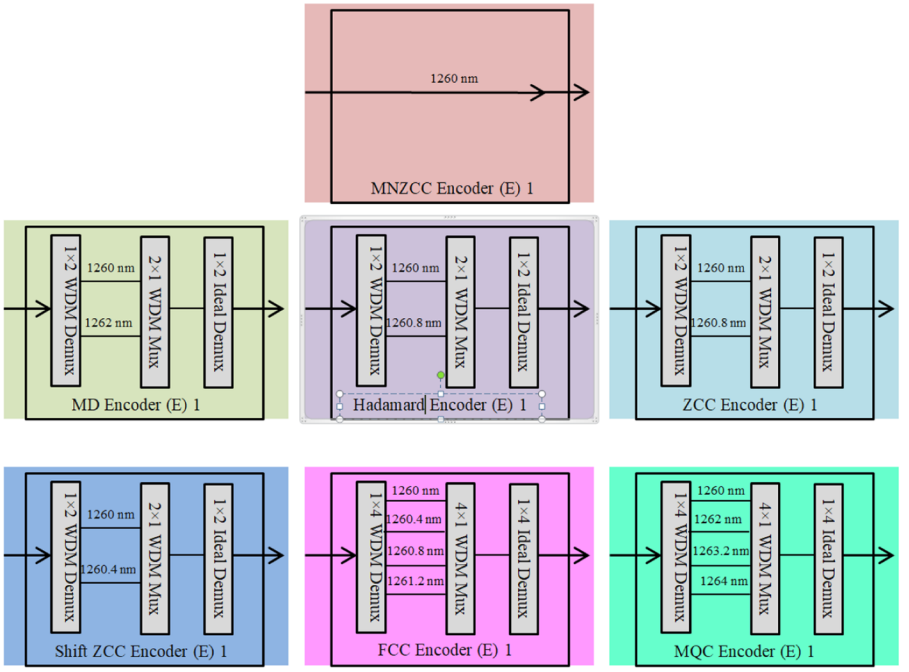

(c)

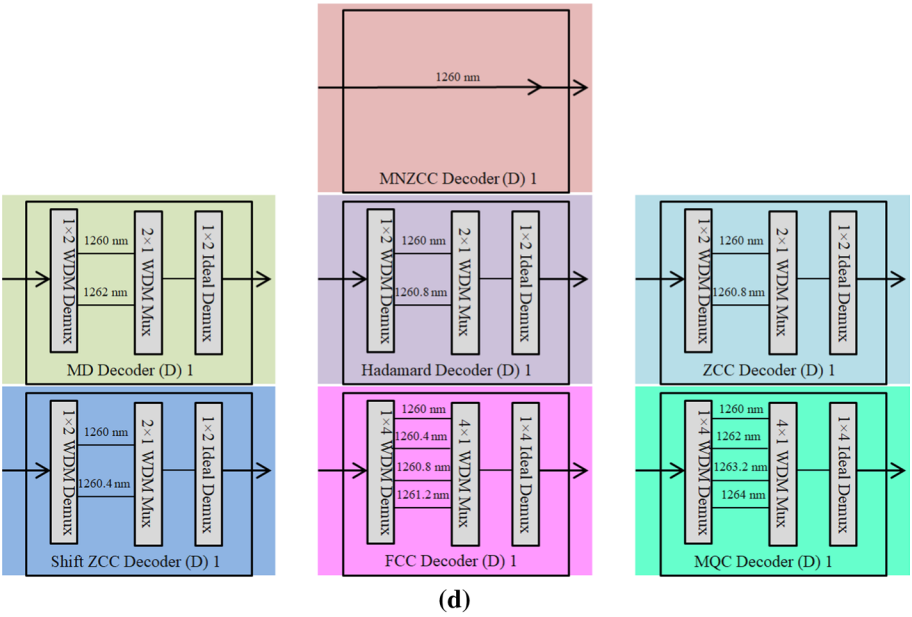

(d)

Fig. 2 (continued)

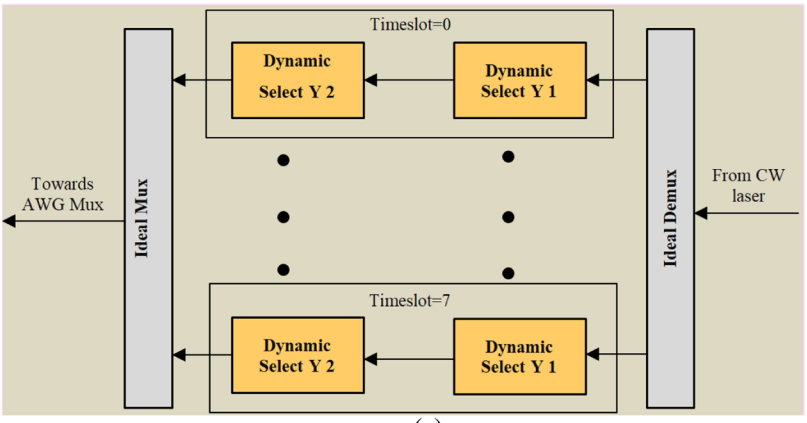

(e)

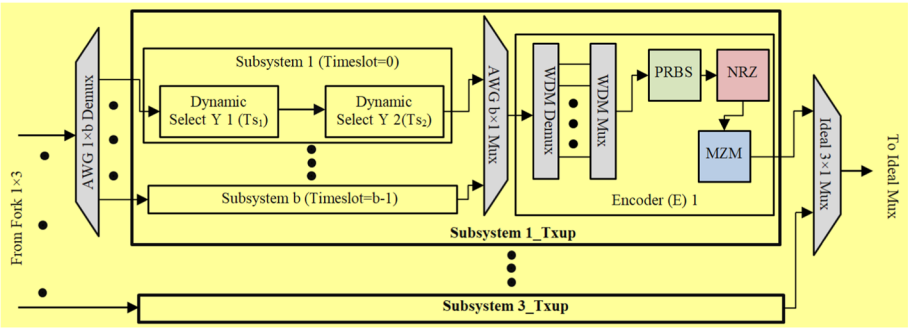

(f)

Fig. 2 (continued)

specific wavelength and to regenerate the distorted signal respectively. BER analyser is used to analyse the performance of the system in terms of quality (Q) factor, BER, eye diagrams, threshold etc.(Cao and Gan 2012; Kachhatiya and Prince 2016; Mostafa and Mohamed 2017; Nyachionjeka and Makondo 2014; Rashidi[a] et al. 2013; Wei et al. 2001).

For upstream, the hybrid WDM-OCDMA-PON system employing MNZCC code consists of 32 ONUs depends upon the code design. Here, each ONUs tuned using y number of CW lasers (1260–1264.4 nm, spectral width = 0.4 nm, $P_{in} = 0$ dBm) by using MZM modulator at 2.5 Gbps NRZ-PRBS data signal, as shown in Fig. 2a. The decoder design of different codes is shown in Fig. 2d. Two cascaded dynamic Y selects are used with different switching time (0 ns to 1.6 ns, with time slot from 0 to 7), for each wavelength as shown in Fig. 2e. The y wavelengths multiplexed by $y \times 1$ AWG multiplexer followed by 1×3 Fork and forwarded into four corresponding groups from Subsystem 1_Txup to Subsystem 3_Txup. Here, each Subsystem comprises a $y \times 1$ AWG demultiplexer, y Subsystems for distinct time switching of signals using two dynamic Y selects. Finally the signals are passed through 4×1 ideal multiplexer for detection and analysis of received signals as shown in Fig. 2f. The switching time T_1 and T_2 for two cascaded dynamic selects Y1 and Y2 are given as (Kumari et al. 2019):

Table 2 Hadamard, MD and ZCC codes for three subscribers (Bhanja and Panda 2017; Hussein et al. 2011; Nisar et al. 2019; Panda 2017; Rashidi et al. 2010; Rashidi[a] et al. 2013; Samanta et al. 2019; Wei et al. 2001)

Code	Hadamard			MD			ZCC		
$\lambda_{dn}/\lambda_{up}$ (nm)	s_1	s_2	s_3	s_1	s_2	s_3	s_1	s_2	s_3
1575/1260	1	1	1	1	0	0	1	0	0
1575.4/1260.4	0	1	0	0	1	0	0	1	0
1575.8/1260.8	1	0	0	0	0	1	1	0	0
1576.2/1261.2	0	0	1	0	0	1	0	0	1
1576.6/1261.6				0	1	0	0	1	0
1577/1262				1	0	0	0	0	1

Table 3 Shift ZCC, FCC, MNZCC and MQC codes for three subscribers (Bhanja and Panda 2017; Hussein et al. 2011; Nisar et al. 2019; Panda 2017; Rashidi et al. 2010; Rashidi[a] et al. 2013; Samanta et al. 2019; Wei et al. 2001)

Code	Shift ZCC			FCC			MNZCC			MQC		
$\lambda_{dn}/\lambda_{up}$ (nm)	s_1	s_2	s_3	s_1	s_2	s_3	s_1	s_2	s_3	s_1	s_2	s_3
1575/1260	1	0	0	1	0	0	0	0	1	1	0	1
1575.4/1260.4	1	0	0	1	0	0	0	1	0	0	1	0
1575.8/1260.8	0	1	0	1	0	0	1	0	0	0	0	0
1576.2/1261.2	0	1	0	1	1	0				0	1	0
1576.6/1261.6	0	0	1	0	1	0				0	0	1
1577/1262	0	0	1	0	1	0				1	0	0
1577.4/1262.4				0	1	1				0	1	1
1577.8/1262.8				0	0	1				0	0	1
1578.2/1263.2				0	0	1				1	0	0
1578.6/263.6				0	0	1				0	0	0
1579/1264										1	1	0
1579.4/1264.4										0	0	0

$$T_1 = \mathrm{TS} \cdot \left(\frac{1}{\text{Data rate}}\right) \cdot \left(\frac{\mathrm{SL}}{s_u}\right) \tag{25}$$

and

$$T_2 = \mathrm{TS} \cdot \left(\frac{1}{\text{Data rate}}\right) \cdot \left(\frac{\mathrm{SL}}{s_u}\right) + \left(\frac{\text{Time window}}{s_u}\right) \tag{26}$$

where TS, SL and TW present the timeslot (0–7), sequence length (128) and time window (1.28×10^{-08} s). s_u denotes the number of upstream subscribers using the single upstream frequency at 1550 nm reference wavelength. The code designs of Hadamard, MD, ZCC, shift ZCC, FCC, MNZCC and MQC codes for three downstream and upstream users are presented in both Tables 2 and 3.

Also, the chip positions for various OCDMA codes used in proposed design is as follows (Bhanja and Panda 2017; Hussein et al. 2011; Nisar et al. 2019; Panda 2017; Rashidi et al. 2010; Rashidi[a] et al. 2013; Samanta et al. 2019; Wei et al. 2001):

MNZCC code

$$chip\ positions = \begin{cases} Subsciber\ 1 \rightarrow 3 \\ Subsciber\ 2 \rightarrow 2 \\ Subsciber\ 3 \rightarrow 4 \end{cases} \tag{27}$$

MD code

$$chip\ positions = \begin{cases} Subsciber\ 1 \rightarrow 1, 6 \\ Subsciber\ 2 \rightarrow 2, 5 \\ Subsciber\ 3 \rightarrow 3, 4 \end{cases} \tag{28}$$

Hadamard code

$$chip\ positions = \begin{cases} Subsciber\ 1 \rightarrow 1, 3 \\ Subsciber\ 2 \rightarrow 1, 2 \\ Subsciber\ 3 \rightarrow 1, 4 \end{cases} \tag{29}$$

ZCC code

$$chip\ positions = \begin{cases} Subsciber\ 1 \rightarrow 1, 3 \\ Subsciber\ 2 \rightarrow 2, 5 \\ Subsciber\ 3 \rightarrow 4, 6 \end{cases} \tag{30}$$

Shift ZCC code

$$chip\ positions = \begin{cases} Subsciber\ 1 \rightarrow 1, 2 \\ Subsciber\ 2 \rightarrow 3, 4 \\ Subsciber\ 3 \rightarrow 5, 6 \end{cases} \tag{31}$$

FCC code

$$chip\ positions = \begin{cases} Subsciber\ 1 \rightarrow 1, 2, 3, 4 \\ Subsciber\ 2 \rightarrow 4, 5, 6, 7 \\ Subsciber\ 3 \rightarrow 7, 8, 9, 10 \end{cases} \tag{32}$$

MQC code

$$chip\ positions = \begin{cases} Subsciber\ 1 \rightarrow 1, 6, 9, 11 \\ Subsciber\ 2 \rightarrow 2, 4, 7, 11 \\ Subsciber\ 3 \rightarrow 1, 5, 7, 8 \end{cases} \tag{33}$$

Table 4 shows the parameters used for the proposed hybrid WDM-OCDMA PON system using integrated fiber-FSO link.

Table 4 Parameters used for hybrid WDM-OCDMA PON system with integrated fiber-FSO link (Gan and Cao 2011; Kachhatiya and Prince 2016)

Parameters	Value
Transmission rate per channel	
Downlink	10 Gbps
Uplink	2.5 Gbps
Mux and Demux bandwidth	0.16 nm
WDM-OCDMA channel spacing	0.4 nm
Responsivity	0.9 A/W
Dark current	10 nA
Thermal noise	1×10^{-22} W/Hz
Cut off frequency	
Uplink	1.87 GHz
Downlink	7.5 GHz
Reference wavelength	1550 nm
Circulator return loss	65 dB
Fiber	
Dispersion	17 ps/nm-km
Attenuation	0.2 dB/km
Fiber length	10–60 km
Dispersion slope	0.075 ps/nm^2/km
FSO	
Range	10–500 m
Attenuation	
Clear air	0.2 dB/km
Haze	2.8 dB/km
Rain	6.5 dB/km
Dust-fog	14.7 dB/km

4 Result and analysis

In this paper, the simulated performance analysis of a full-duplex hybrid WDM-OCDMA PON employing different OCDMA codes over hybrid fiber-FSO link is presented using Optisystem v.18. Here, the performance of the system is measured at 1575 nm and 1260 nm wavelengths for WDM-OCDMA PON downstream and upstream transmission respectively. Again, the performance of the proposed system is analysed in terms of Q value, log(BER), eye diagrams, received optical power ($P_{r)}$ in dB and SNR in dB under the impact of weak turbulence condition with distinct climate conditions, shot noise and thermal noise. Here, the fiber length, FSO range, FSO receiver and FSO transmitter aperture diameter are considered as 10 km, 10 m, 10 cm and 10 cm respectively.

In Fig. 3a the performance of the proposed WDM-OCDMA PON with MNZCC code over fiber-FSO link with regards the FSO range for both upstream and downstream transmission under the impact of clear air, haze, rain and dust-fog atmospheric conditions is evaluated. From figure it is observed that as the FSO channel range increases, the incoming coded signal would diverge gradually. From simulation result, when the downstream FSO length is 100, 300 and 500 m the observed Q-factor is 29, 15 and 1 for clear air respectively. For the same FSO link, the obtained Q-factor for haze Q value is 28, 13 and 0, for rain is 26, 9 and 0 as well as for dust-fog is 25, 7 and 0 over 100, 300 and 500 m respectively.

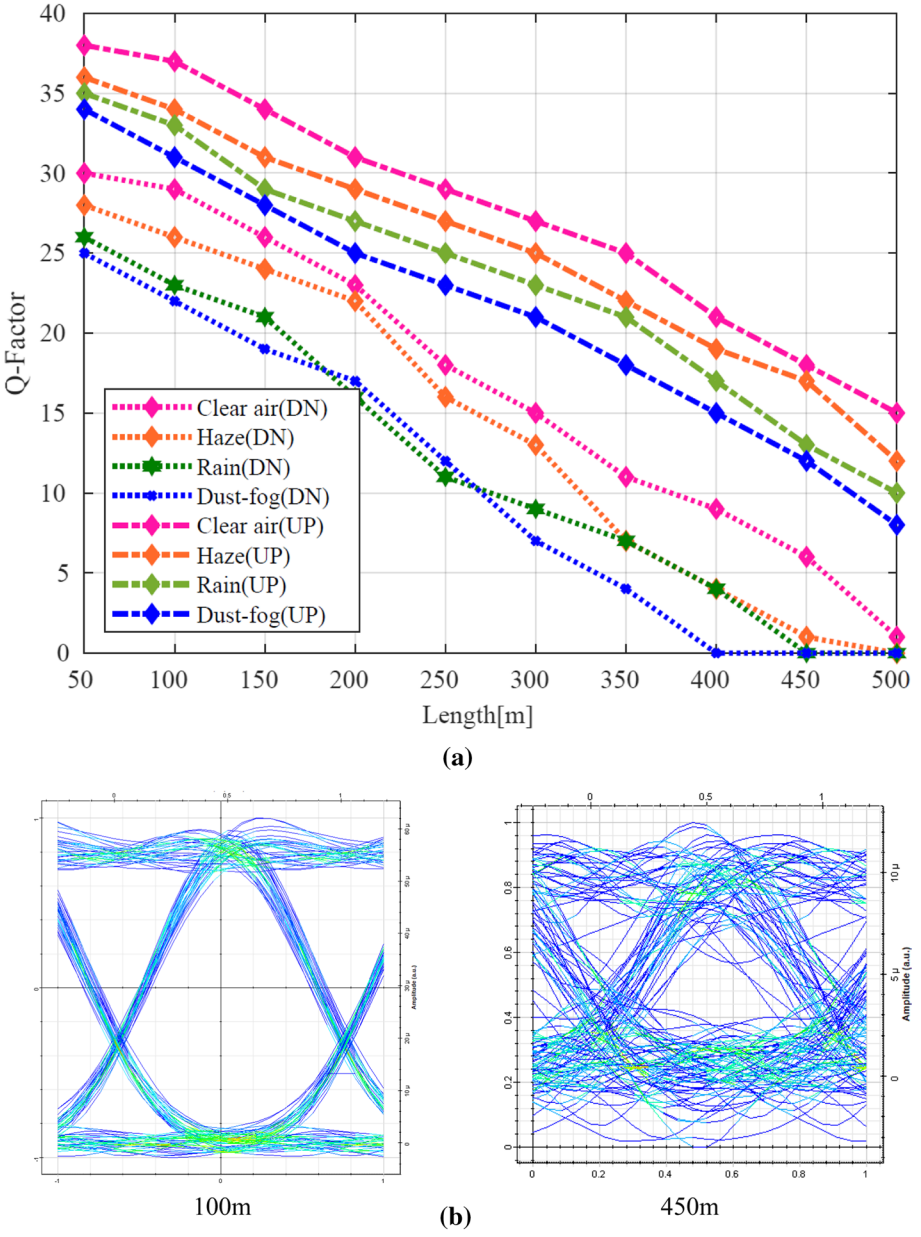

Fig. 3 Calculated Q-Factor vs. FSO range under clear air, haze, rain and dust-fog for both **a** downstream and upstream transmission, eye diagrams of FSO signals for **b** downstream and **c** upstream transmission at 100 and 450 m FSO distance under clear air climate condition

Again for the upstream FSO range, the noted Q-factor is 37, 27 and 15 for clear air; 36, 25 and 12 for haze; 35, 23 and 10 for rain and 34, 21 and 8 for dust-for over 100, 300 and 500 m FSO length respectively. It is also seen that hybrid fiber-FSO (10 km + 50–500 m)

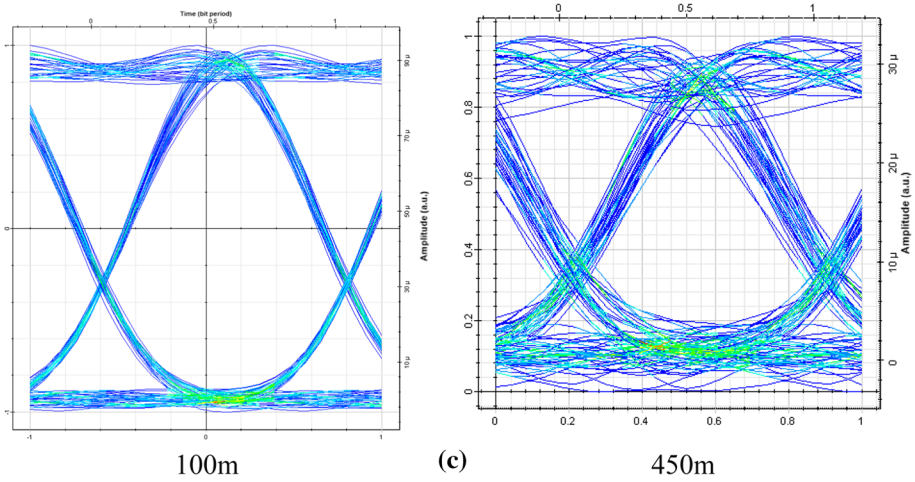

Fig. 3 (continued)

performs superior with acceptable Q factor (≥ 6) under clear air followed by haze, rain and dust-fog for both uplink and downlink transmission. However, uplink FSO link performs better than downstream due to presence of low input power (0dBm) and low data rate (2.5Gbps) in uplink transmission system. Thus the maximum faithful FSO ranges for downstream and upstream channel are 450 and 600 m for clear air; 350 and 550 m for haze; 330 m and 520 m for rain as well as 300 m and 500 m for dust-fog respectively.

Figure 3b and c presents the eye diagrams over 100 and 450 m for both downstream and upstream transmission respectively. The open eye diagrams show the feasibility of the proposed WDM-FSO-OCDMA PON system under clear weather condition at 10/2.5Gbps per channel bidirectional transmission. However, the closed eyes indicate the effect of fiber non-linearities, ISI and MAI due to different no. users (Mrabet 2020). The comparative analysis of the proposed hybrid system employing MNZCC code with hybrid fiber-FSO links for downlink/uplink transmission for varying FSO range under different weather conditions is tabulated in Table 5.

The above-reported results illustrate that the proposed PON system for varying FSO range performs best under clear air environment conditions followed by haze, rain and dust-fog for both downlink and uplink transmission.

The number of active users retrieving the proposed system is a significant performance measure of the hybrid fiber-FSO link. The measured no. of users vs. log(BER) for downstream and upstream different OCDMA codes' signals under clear air is presented in Fig. 4a and b respectively. From both figures it can be seen that when the number of end users retrieving the system increases, the system noise level especially due to MAI and shot noises, increases consequently and system transmission performance declines. Further, when the system employs MNZCC code, when the deciding threshold of the receiver is fix as the superior and log(BER) is at -9 magnitude, most of users can retrieve the system successfully. While when the system uses shift ZCC, MD, MQC, ZCC, Hadamard and FCC codes, only few of the users can reacquire the system. Thus for downstream transmission, MNZCC code can support maximum users upto 100 users [log(BER) = -9] followed by 95 by MD, 95 by shift ZCC, 90 by Hadamard, 90 by ZCC, 75 by MQC and 70 by FCC as shown in Fig. 4a.

Table 5 Comparative performance analysis of downlink and uplink hybrid fiber-FSO links for varying FSO range under different environment conditions

	Downlink						Uplink					
FSO range (m)	100		300		500		100		300		500	
Climate	log (BER)	ROP (dBm)	log (BER)	ROP (dBm)	log (BER)	ROP (dBm)	log (BER)	ROP (dBm)	log (BER)	ROP (dBm)	log (BER)	ROP (dBm)
Clear air	−40	3	−33	1	−31	−4	−44	5	−35	3	−32	−2
Haze	−37	−1	−29	−2	−25	−10	−40	1	−31	0	−26	−6
Rain	−31	−5	−26	−7	−21	−14	−37	−2	−28	−3	−24	−10
Dust-fog	−20	−9	−24	−11	−19	−17	−27	−6	−26	−8	−22	−14

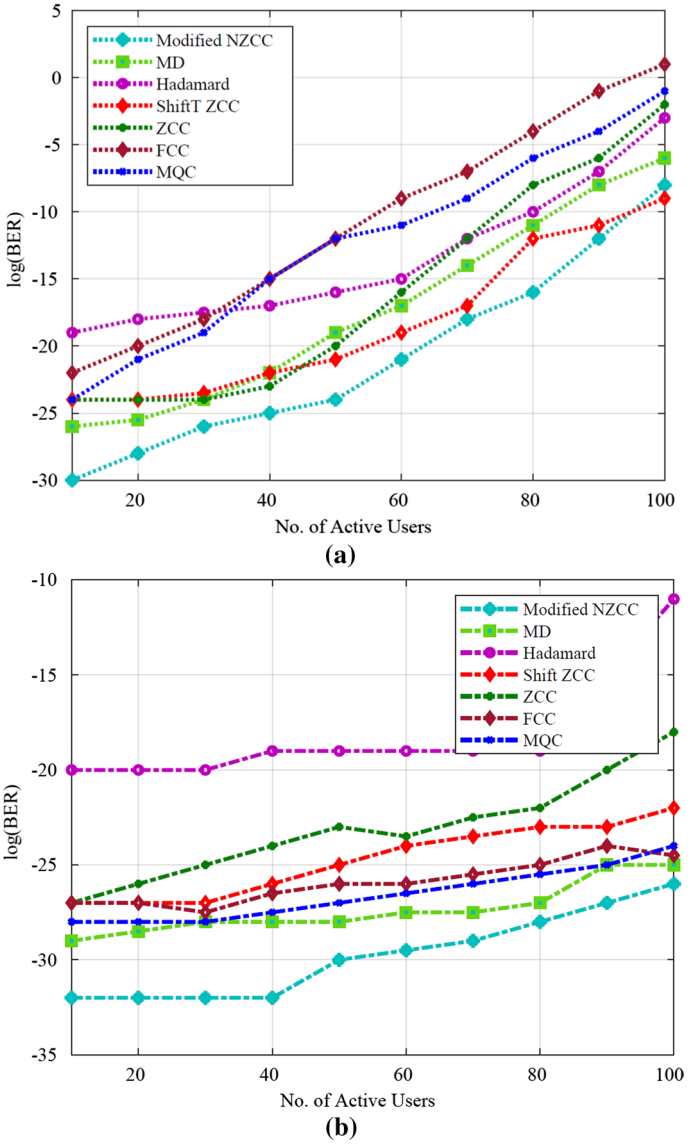

Fig. 4 Measured no. of users vs. log(BER) for **a** downstream and **b** upstream under clear air using different codes

While for uplink transmission, MNZCC code can support more than 100 users [log(BER) = −26] simultaneously followed by MD, FCC, MQC, shift ZCC, ZCC and Hadamard as shown in Fig. 4b. Hence, MNZCC code shows better preformance than other code over upstream hybrid fiber-FSO link than other codes. The comparative analysis of the proposed work employing different codes with hybrid fiber-FSO links for varying no. of users in downlink/uplink transmission under clear air climate condition is tabulated in Table 6.

Table 6 Comparative performance analysis of downlink and uplink hybrid fiber-FSO links (10 km + 10 m) for varying no. of subscribers' using different OCDMA codes under clear air environment condition

	Downlink						Uplink					
No. of users	10		50		100		10		50		100	
Code	log (BER)	ROP (dBm)	log (BER)	ROP (dBm)	log (BER)	ROP (dBm)	log (BER)	ROP (dBm)	log (BER)	ROP (dBm)	log (BER)	ROP (dBm)
MNZCC	−30	3	−29	−5	−21	−12	−32	5	−30	−2	−26	−8
MD	−26	−1	−26	−8	−22	−17	−29	1	−28	−5	−23	−12
Hadamard	−18	−5	−17	−12	−09	−22	−20	−3	−19	−9	−10	−16
Shift ZCC	−25	−9	−24	−16	−16	−27	−27	−7	−25	−13	−18	−20
ZCC	−24	−13	−23	−20	−14	−32	−27	−11	−23	−17	−15	−24
FCC	−26	−17	−25	−24	−20	−35	−27	−15	−26	−21	−23	−28
MQC	−27	−20	−26	−28	−22	−39	−28	−18	−27	−24	−23	−32

The above-reported results summarized that MNZCC code is most desirable for variable no. of users in both downlink and uplink hybrid fiber-FSO links in terms of minimum BER and high ROP than other codes. Also, uplink transmission shows better performance than downlink transmission.

Figure 5a and b show the graph between log(BER) versus the fiber length for different OCDMA codes for downstream and upstream transmission respectively. From

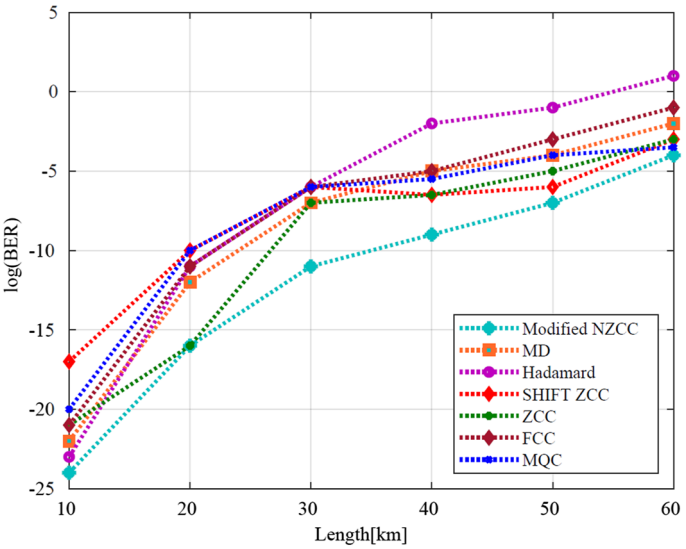

(a)

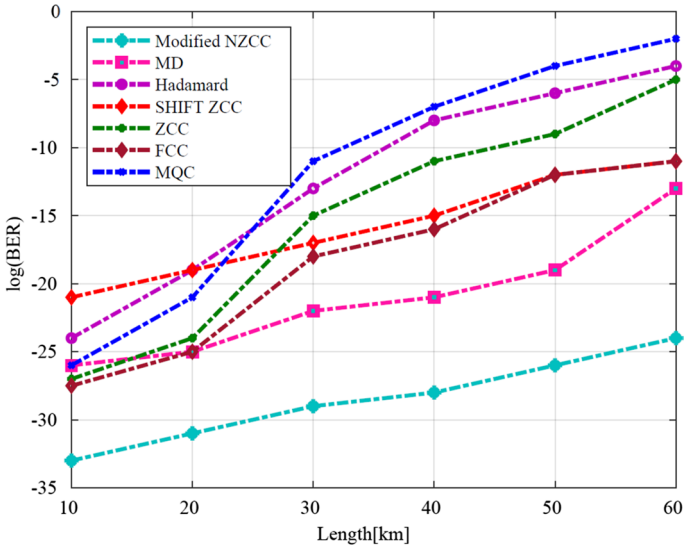

(b)

Fig. 5 Variation of BER with varying fiber lengths for **a** downstream, **b** upstream, eye diagrams of fiber links at 10 and 60 km for **c** downstream and **d** upstream transmission

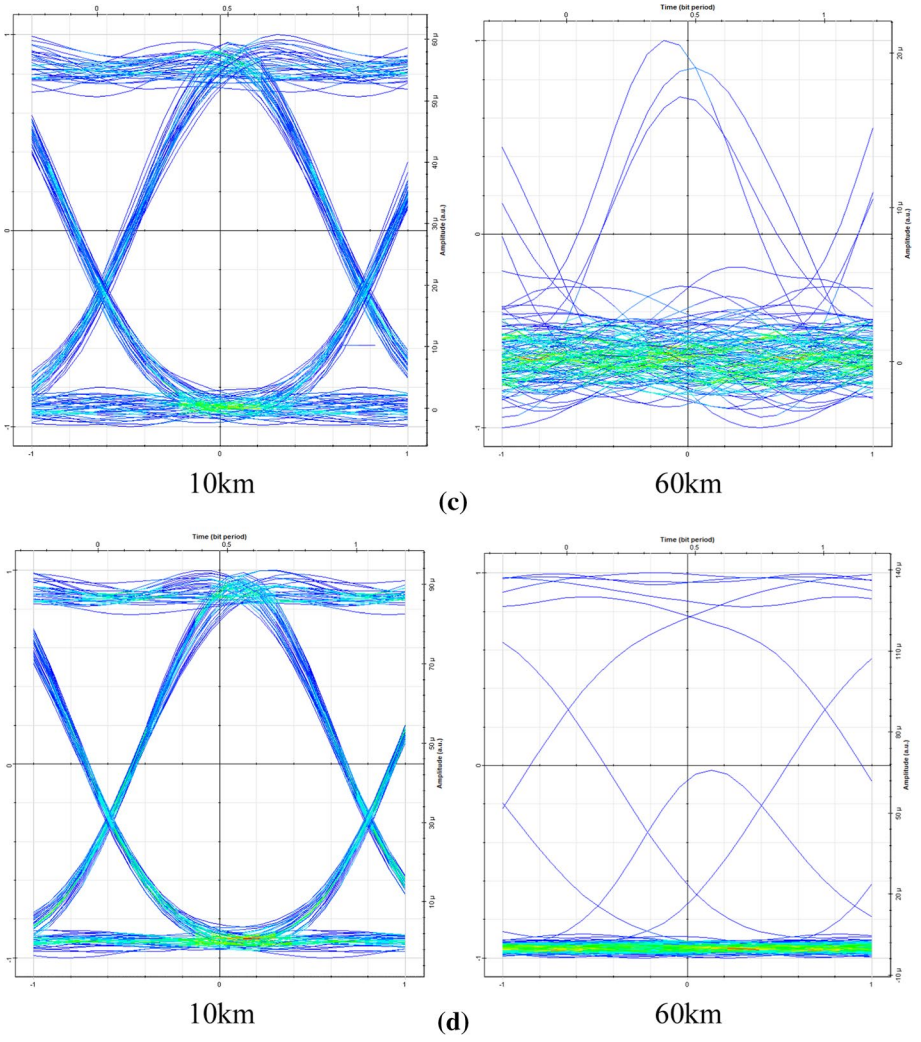

Fig. 5 (continued)

Fig. 5a, it has been seen that there is a considerable increase in the log(BER) values from −24 to −4, −22 to −2, −23 to 1, −17 to −3, −21 to −3, −21 to −1 and −20 to −3.5 for downstream transmission distance from 10 to 60 km in case of MZNCC, MD, Hadamard, shift ZCC, ZCC, FCC and MQC respectively. Similarly Fig. 5b also shows that BER values increases from −33 to −24, −26 to −13, −24 to −4, −21 to −11, −27 to −5, −27.5 to −11 and −26 to −2 for upstream transmission distance from 10 to 60 km in case of MZNCC, MD, Hadamard, shift ZCC, ZCC, FCC and MQC respectively. The increase in BER values w.r.t. length is due to presence of fiber non linearities, ISI, dispersion, attenuation and noise in the system. Besides this, MNZCC code shows superior performance followed by MQC, ZCC, shift ZCC, MD, Hadamard and FCC for downlink transmission. Also, it is observed that uplink transmission performs

better than downlink transmission for different OCDMA code with best performance by MNZCC followed by Hadamard, MD, ZCC, FCC, MQC and shift ZCC.

Figure 5c and d present the eye diagrams over 10 and 60 km for both downstream and upstream transmission respectively. Here, the large eye opening indicates the viability of the proposed WDM-FSO-OCDMA PON system employing MNZCC code under clear weather condition at 10/2.5Gbps per channel bidirectional transmission (Mrabet 2020). The comparative analysis of the proposed work employing different codes with hybrid fiber-FSO links for downlink/uplink transmission under clear air climate condition is tabulated in Table 7.

The above-reported results predict that MNZCC code is most desirable for variable received optical power in both downlink and uplink hybrid fiber-FSO links in terms of minimum BER and high SNR than other codes. Also, uplink transmission shows better performance than downlink transmission.

Tables 8, 9, 10, 11, 12, 13, 14 and 15 show the comparative analysis of the hybrid WDM-OCDMA PON employing MNZCC code with integrated fiber-FSO link (10 km fiber + 10 m FSO) transmitter and receiver aperture diameter of 10 and 20 cm respectively, under the impact of different environment conditions for downstream and upstream transmission. The system performance is compared for varying beam divergence, transmitter loss, receiver loss, and additional loss in terms received power, SNR and log(BER) over 10 km fiber and 10 m FSO range at 10/2.5 Gbps data rate. It is observed that as the beam divergence, transmitter and receiver losses are increases, the performance of the system decreases under different weather conditions. The performance of system can be best achieved under the impact of clear air, followed by haze, rain and dust-fog. Moreover, upstream transmission shows better performance than downstream due to less ISI, low input power as well as data rate than downstream transmission (Table 16).

The comparative analysis of the proposed system employing MNZCC code with other different codes means DCS, MDW, EDW, hadamard and MQC is tabulated in Table 15. From table it is clear that the proposed work at less weight and code length can handle more no. of users with zero cross-correlation. Also, the code construction of MNZCC is simple, hence simple encoder decoder design which reduces the cost of the system. Hence, the bidirectional hybrid WDM-OCDMA PON employing MNZCC code with integrated fiber-FSO link under clear air atmospheric condition offers many benefits like high transmission rate, long-reach transmission, cost-effeteness, easy upgradeability, reliability, scalability and security by supporting a large number of subscribers.

5 Conclusion

A hybrid full-duplex 120/30Gbps WDM-OCDMA PON employing seven OCDMA codes viz. MNZCC, MD, ZCC, hadamard, shift ZCC, FCC and MQC with hybrid fiber-FSO link under different weather conditions over long reach (60 km fiber + 500 m FSO) to allow the information to the wired as well as wireless 68 subscribers is proposed and investigated. Employment of MNZCC code for downlink and uplink transmission in the hybrid fiber-FSO are the primary steps to avoid the transmission impairments like fiber non-linearities, ISI, noise and dispersion under the impact of adverse atmospheric conditions. Integrated fiber-FSO link in proposed system improves the data transmitting capacity, offers 'pay-as-you-grow' features, security and reduce the overall system cost by reducing number of encoders/decoders even in unworkable environment restrictions. Minimum BER value

Table 7 Comparative performance analysis of downlink and uplink hybrid fiber-FSO links employing different OCDMA codes for varying fiber distance under clear air environment conditions

	Downlink						Uplink					
Fiber range (km)	10		30		50		10		30		50	
Code	SNR (dB)	ROP (dBm)	SNR (dB)	ROP (dBm)	SNR (dB)	ROP (dBm)	SNR (dB)	ROP (dBm)	SNR (dB)	ROP (dBm)	SNR (dB)	ROP (dBm)
MNZCC	35	5	33	3	30	3	37	6	35	5	34	4
MD	32	2	29	−1	27	−1	35	4	31	2	29	1
Hadama-rd	31	−2	26	−6	24	−6	33	0	29	−2	25	−4
Shift ZCC	31	−7	27	−10	25	−10	33	−4	29	−8	26	−9
ZCC	30	−11	26	−14	24	−14	32	−7	29	−11	25	−12
FCC	30	−15	27	−18	25	−18	33	−12	29	−16	26	−18
MQC	31	−18	26	−21	24	−21	33	−15	30	−18	25	−23

Table 8 Comparative performance analysis of downlink hybrid fiber-FSO link in the presence of different transmission losses for clear air weather condition

Beam divergence (mrad)	Loss (dB)			WDM-OCDMA		
	Transmitter	Receiver	Additional	Received optical power (dBm)	SNR (dB)	log (BER)
2	1	1	1	0.91	103	−31
2.5	2	2	2	0.89	101	−29
3	3	3	3	0.85	98	−27
3.5	4	4	4	0.81	95	−22
4	5	5	5	0.78	92	−18

Table 9 Comparative performance analysis of downlink hybrid fiber-FSO link in the presence of different transmission losses for haze weather condition

Beam divergence (mrad)	Loss (dB)			WDM-OCDMA		
	Transmitter	Receiver	Additional	Received optical power (dBm)	SNR (dB)	log (BER)
2	1	1	1	0.88	100	−27
2.5	2	2	2	0.84	97	−24
3	3	3	3	0.81	94	−21
3.5	4	4	4	0.77	91	−18
4	5	5	5	0.75	89	−14

Table 10 Comparative performance analysis of downlink hybrid fiber-FSO link in the presence of different transmission losses for rain weather condition

Beam divergence (mrad)	Loss (dB)			WDM-OCDMA		
	Transmitter	Receiver	Additional	Received optical power (dBm)	SNR (dB)	log (BER)
2	1	1	1	0.81	94	−20
2.5	2	2	2	0.77	91	−15
3	3	3	3	0.75	89	−12
3.5	4	4	4	0.72	85	−10
4	5	5	5	0.70	82	−7

(approx. 10^{-9}), high received power (dBm), high Q-factor, eye diagrams and high SNR (dB) also presents maintenance of viability condition of the proposed system. It is analysed that the proposed system performs well under clear air climate condition followed by haze, rain and dust-fog. The results reported that the over the fiber length of 10 km, the long wireless FSO range of 450 m having received power of −4dBm and more than 500 m having received power of −2dBm downlink and uplink transmission can be achieved in the proposed system at 10/2.5Gbps transmission rate under clear air. While under haze,

Table 11 Comparative performance analysis of downlink hybrid fiber-FSO link in the presence of different transmission losses for dust-fog weather condition

Beam divergence (mrad)	Loss (dB)			WDM-OCDMA		
	Transmitter	Receiver	Additional	Received optical power (dBm)	SNR (dB)	log (BER)
2	1	1	1	0.72	85	−10
2.5	2	2	2	0.70	82	−7
3	3	3	3	0.67	79	−3
3.5	4	4	4	0.64	75	1
4	5	5	5	0.61	73	1

Table 12 Comparative performance analysis of uplink hybrid fiber-FSO link in the presence of different transmission losses for clear air weather condition

Beam divergence (mrad)	Loss (dB)			WDM-OCDMA		
	Transmitter	Receiver	Additional	Received optical power (dBm)	SNR (dB)	log (BER)
2	1	1	1	0.95	105	−33
2.5	2	2	2	0.92	103	−31
3	3	3	3	0.88	101	−29
3.5	4	4	4	0.86	98	−27
4	5	5	5	0.82	95	−22

Table 13 Comparative performance analysis of uplink hybrid fiber-FSO link in the presence of different transmission losses for haze weather condition

Beam divergence (mrad)	Loss (dB)			WDM-OCDMA		
	Transmitter	Receiver	Additional	Received optical power (dBm)	SNR (dB)	log (BER)
2	1	1	1	0.90	100	−27
2.5	2	2	2	0.87	97	−25
3	3	3	3	0.86	94	−21
3.5	4	4	4	0.85	91	−18
4	5	5	5	0.82	89	−15

rain and dust-fog atmospheric condition, the maximum achieved FSO range are 350, 330 and 300 m for downstream and 550, 520, 500 m for upstream respectively. In addition, the comparative analysis of the proposed system using distinct OCDMA codes over 10 km fiber and 10 m FSO range demonstrate that modified NZCC code performs superior than other codes in terms of handling 100 no. of users in downlink and even more than this for uplink transmission at received power of −12 and −8 dBm respectively at log(BER) of −9. Moreover, for the hybrid fiber-FSO link (10 m + 60 km) range, the proposed system employing modified NZCC code provides quite high SNR of 30 dB and 34 dB at downstream received power of 3dBm and upstream received power of 4dBm respectively. The

Table 14 Comparative performance analysis of uplink hybrid fiber-FSO link in the presence of different transmission losses for rain weather condition

Beam divergence (mrad)	Loss (dB)			WDM-OCDMA		
	Transmitter	Receiver	Additional	Received optical power (dBm)	SNR (dB)	log (BER)
2	1	1	1	0.87	93	−20
2.5	2	2	2	0.84	90	−15
3	3	3	3	0.81	88	−11
3.5	4	4	4	0.78	83	−7
4	5	5	5	0.74	80	−5

Table 15 Comparative performance analysis of uplink hybrid fiber-FSO link in the presence of different transmission losses for dust-fog weather condition

Beam divergence (mrad)	Loss (dB)			WDM-OCDMA		
	Transmitter	Receiver	Additional	Received optical power (dBm)	SNR (dB)	log (BER)
2	1	1	1	0.81	88	−11
2.5	2	2	2	0.78	83	−7
3	3	3	3	0.74	80	−5
3.5	4	4	4	0.71	78	−2
4	5	5	5	0.68	75	−1

Table 16 Performance comparison of the proposed PON system with different OCDMA codes

References	OCDMA code	Weight (w)	Code length (l)	Number of subscribers (s)	Cross-correlation
Jellali et al. (2017)	DCS	4	30	30	≤ 1
El-Mottaleb et al. (2020)	MDW	4	90	30	≤ 1
Kumawat and Ravi Kumar (2016)	EDW	4	30	10	≤ 1
Samanta et al. (2019)	Hadamard	16	32	30	≤ 1
Wei et al. (2001)	MCQ	6	30	25	1
Proposed system	MNZCC	4	24	36	0

beam divergence, transmitter and receiver losses are also measured for different weather conditions over the integrated fiber-FSO link (10 km fiber + 10 m FSO) to check and determine the best possible performance of system for both downstream and upstream transmission. On comparison with other exiting previous work, the hybrid 160/40Gnps full-duplex WDM-OCDMA PON employing modified NZCC code expresses the potential to handle large no. of users, long-reach transmission, data rate and security. Therefore the advantages of channelization, integration and low power consumption of hybrid WDM-FSO-OCDMA PON offer a promising result on constructing the next generation fronthaul/backhaul integrated wired-wireless links.

Authors' contributions All authors contributed to the study conception and design. All authors read and approved the final manuscript.

Funding Not applicable.

Availability of data and materials Not applicable.

Declarations

Conflict of interest The authors declare no competing interests.

Ethical approval Not applicable.

References

Al-Khafaji, H.M.R., Aljunid, S.A., Fadhil, H.A.: Improved BER based on intensity noise alleviation using developed detection technique for incoherent SAC-OCDMA systems. J. Mod. Opt. **59**, 878–886 (2012). https://doi.org/10.1080/09500340.2012.676094

Alsharif, M.H., Nordin, R., Abdullah, N.F., Kelechi, A.H.: How to make key 5G wireless technologies environmental friendly: A review. Trans. Emerg. Telecommun. Technol. **29**, 1–32 (2018). https://doi.org/10.1002/ett.3254

Amphawan, A., Chaudhary, S., Chan, V.: Optical millimeter wave mode division multiplexing of LG and HG modes for OFDM Ro-FSO system. Opt. Commun. **431**, 245–254 (2019). https://doi.org/10.1016/j.optcom.2018.07.054

Anuar, M.S., Aljunid, S.A., Saad, N.M., Hamzah, S.M.: New design of spectral amplitude coding in OCDMA with zero cross-correlation. Opt. Commun. **282**, 2659–2664 (2009). https://doi.org/10.1016/j.optcom.2009.03.079

Anuranjana, Kaur, S., Goyal, R., Chaudhary, S.: 1000 Gbps MDM-WDM FSO link employing DP-QPSK modulation scheme under the effect of fog. Optik (Stuttg). 257, 168809 (2022). https://doi.org/10.1016/j.ijleo.2022.168809

Bhanja, U., Panda, S.: Comparison of novel coding techniques for a fixed wavelength hopping SAC-OCDMA. Photonic Netw. Commun. **33**, 179–193 (2017). https://doi.org/10.1007/s11107-016-0632-5

Cao, Y., Gan, C.: A scalable hybrid WDM/OCDMA-PON based on wavelength-locked RSOA technology. Optik (Stuttg). **123**, 176–180 (2012). https://doi.org/10.1016/j.ijleo.2011.03.015

Cena, G., Valenzano, A., Vitturi, S.: Hybrid wired/wireless networks for real-time communications. Ind. Electron. **2**, 8–20 (2008)

Chaudhary, S., Tang, X., Wei, X.: Comparison of Laguerre-Gaussian and Donut modes for MDM-WDM in OFDM-Ro-FSO transmission system. AEU - Int. J. Electron. Commun. **93**, 208–214 (2018). https://doi.org/10.1016/j.aeue.2018.06.024

Ciaramella, E., Arimoto, Y., Contestabile, G., Presi, M., D'Errico, A., Guarino, V., Matsumoto, M.: 1.28-Tb/s (32 × 40 Gb/s) Free-space optical WDM transmission system. IEEE Photonics Technol. Lett. **21**, 1121–1123 (2009). https://doi.org/10.1109/LPT.2009.2021149

Curri, V., Capriata, S., Gaudino, R.: Outage probability due to stimulated raman scattering in GPON and TWDM-PON coexistence. In: Optical Fiber Communication Conference (2014)

Dayal, N., Singh, P., Kaur, P.: Long range cost-effective WDM-FSO system using hybrid optical amplifiers. Wirel. Pers. Commun. **97**, 6055–6067 (2017). https://doi.org/10.1007/s11277-017-4826-7

Dutta, B., Kuiri, B., Santra, S., Sarkar, N., Biswas, I.A., Atta, R., Patra, A.S.: 100 Gbps Data Transmission Based on Different l-valued OAM beam multiplexing employing wdm techniques and free space optics. Opt. Quantum Electron. **53**, (2021). https://doi.org/10.1007/s11082-021-03154-w

Dutta, B., Sarkar, N., Atta, R., Kuiri, B., Santra, S., Patra, A.S.: 640 Gbps FSO data transmission system based on orbital angular momentum beam multiplexing employing optical frequency comb. Opt. Quantum Electron. **54**, (2022). https://doi.org/10.1007/s11082-021-03509-3

Effenberger, F., Lin, H.: Backward compatible coexistence of PON systems. In: Optical Fiber Communication Conference and National Fiber Optic Engineers Conference (2009)

El-Mottaleb, S.A.A., Fayed, H.A., Ismail, N.E., Aly, M.H., Rizk, M.R.M.: MDW and EDW/DDW codes with AND subtraction/single photodiode detection for high performance hybrid SAC-OCDMA/OFDM system. Opt. Quantum Electron. **52**, (2020). https://doi.org/10.1007/s11082-020-02357-x

Fazea, Y.: Mode division multiplexing and dense WDM-PON for fiber-to-the-home. Optik (Stuttg). **183**, 994–998 (2019). https://doi.org/10.1016/j.ijleo.2019.02.072

Gan, C.Q., Cao, Y.N.: Novel architecture of WDM/OCDMA-PON based on SSFBG and wavelength re-modulation technology. J. Shanghai Univ. **15**, 96–100 (2011). https://doi.org/10.1007/s11741-011-0700-3

Hussein, T., Aljunid, S.A., Adnan, H., Ahmad, R.A., Saad, N.M.: Optical Fiber Technology Development of a new code family based on SAC-OCDMA system with large cardinality for OCDMA network. Opt. Fiber Technol. **17**, 273–280 (2011). https://doi.org/10.1016/j.yofte.2011.04.002

Huszaník, T., Turán, J., Ovseník, Ľ: Simulation of Downlink of 10G-PON FTTH in the city of Košice. Carpathian J. Electron. Comput. Eng. **11**, 33–39 (2018). https://doi.org/10.2478/cjece-2018-0006

Jellali, N., Najjar, M., Ferchichi, M., Rezig, H.: Development of new two-dimensional spectral/spatial code based on dynamic cyclic shift code for OCDMA system. Opt. Fiber Technol. **36**, 26–32 (2017). https://doi.org/10.1016/j.yofte.2017.02.002

Ji, J., Wu, B., Zhang, J., Xu, M., Wang, K.: Design and investigation of 10 Gb/s FSO Wiretap channel using OCDMA time-diversity reception. IEEE Photonics J. **12**, 1–12 (2020). https://doi.org/10.1109/JPHOT.2020.2985747

Jiao, W., Liu, H., Yin, J., Wei, Z., Luo, A., Deng, D.: Performance of a QAM/FSO communication system employing spatial diversity in weak and saturation turbulence channels. J. Mod. Opt. **66**, 965–975 (2019). https://doi.org/10.1080/09500340.2019.1596321

Kachhatiya, V., Prince, S.: Four-fold increase in users of time-wavelength division multiplexing (TWDM) passive optical network (PON) by delayed optical amplitude modulation (AM) upstream. Opt. Fiber Technol. **32**, 71–81 (2016)

Kakati, D., Arya, S.C.: Performance of 120 Gbps single channel coherent DP-16-QAM in terrestrial FSO link under different weather conditions. Optik (Stuttg). **178**, 1230–1239 (2019). https://doi.org/10.1016/j.ijleo.2018.10.035

Kumar, N., Singh, T.: 2.50 Gbit/s optical CDMA over FSO communication system. Optik (Stuttg). **125**, 4538–4542 (2014). https://doi.org/10.1016/j.ijleo.2014.02.011

Kumari, M., Sharma, R., Sheetal, A.: Comparative analysis of high speed 20/20 Gbps for long-reach NG-PON2. J. Opt. Commun., 1–14 (2019)

Kumawat, S., Ravi Kumar, M.: Generalized optical code construction for enhanced and Modified Double Weight like codes without mapping for SAC-OCDMA systems. Opt. Fiber Technol. **30**, 72–80 (2016). https://doi.org/10.1016/j.yofte.2016.03.004

Li, C.Y., Huang, X.H., Lu, H.H., Huang, Y.C., Huang, Q.P., Tu, S.C.: A WDM PAM4 FSO-UWOC integrated system with a channel capacity of 100 Gb/s. J. Light. Technol. **38**, 1766–1776 (2020). https://doi.org/10.1109/JLT.2019.2960525

Mandal, G.C., Mukherjee, R., Das, B., Patra, A.S.: A full-duplex WDM hybrid fiber-wired/fiber-wireless/fiber-VLC/fiber-IVLC transmission system based on a self-injection locked quantum dash laser and a RSOA. Opt. Commun. **427**, 202–208 (2018). https://doi.org/10.1016/j.optcom.2018.06.048

Moghaddasi, M., Mamdoohi, G., Muhammad Noor, A.S., Mahdi, M.A., Ahmad Anas, S.B.: Development of SAC-OCDMA in FSO with multi-wavelength laser source. Opt. Commun. **356**, 282–289 (2015). https://doi.org/10.1016/j.optcom.2015.07.075

Mostafa, S., Mohamed, A.E.A.: Performance evaluation of SAC-OCDMA system in free space optics and optical fiber system based on different types of codes. Wirel. Pers. Commun. **96**, 2843–2861 (2017). https://doi.org/10.1007/s11277-017-4327-8

Mrabet, H.: A performance analysis of a hybrid OCDMA-PON configuration based on IM/DD fast-OFDM technique for access network. Appl. Sci. **10**, 1–13 (2020). https://doi.org/10.3390/app10217690

Mukherjee, R., Mallick, K., Kuiri, B., Santra, S., Dutta, B., Mandal, P., Patra, A.S.: PAM-4 based long-range free-space-optics communication system with self injection locked QD-LD and RS codec. Opt. Commun. 476, 126304 (2020a)(a). https://doi.org/10.1016/j.optcom.2020a.126304

Mukherjee, R., Mallick, K., Mandal, P., Dutta, B., Kuiri, B., Patra, A.S.: Bidirectional hybrid OFDM based free-space/wireless-over-fiber transport system. Opt. Quantum Electron. **52**, (2020b). https://doi.org/10.1007/s11082-020-02428-z

Naqshbandi, F., Jha, R.K.: TWDM-PON-AN optical backhaul solution for hybrid optical wireless networks. J. Mod. Opt. **63**, 1899–1916 (2016). https://doi.org/10.1080/09500340.2016.1177126

Nisar, K.S., Sarangal, H., Thapar, S.S.: Performance evaluation of newly constructed NZCC for SAC-OCDMA using direct detection technique. Photonic Netw. Commun. **37**, 75–82 (2019). https://doi.org/10.1007/s11107-018-0794-4

Nyachionjeka, K., Makondo, W.: Effects of modulation techniques (Manchester Code, NRZ or RZ) on the Operation of Hybrid WDM/TDM Passive Optical Networks. Int. Sch. Res. Not. **2014**, 1–8 (2014)
Panda, S.: Effect of SHIFTZCC codes for optical CDMA system. World Sci. News. **67**, 365–389 (2017)
Rashidi, C.B.M., Anuar, M.S., Aljunid, S.A.: Study of direct detection technique for zero cross correlation code in OCDMA. In: Int. Conf. Comput. Commun. Eng. ICCCE'10. 11–13 (2010). https://doi.org/10.1109/ICCCE.2010.5556830
Rashidia, C.B.M., Aljunid, S.A., Ghani, F., Fadhil, H.A., Anuar, M.S.: New Design of Flexible Cross Correlation (FCC) Code for SAC-OCDMA System. Procedia Eng. **53**, 420–427 (2013). https://doi.org/10.1016/j.proeng.2013.02.055
Ratnam, J., Chakrabarti, S., Datta, D.: A heuristic approach for designing hybrid PONs employing WDM and OCDMA with asymmetric traffic distribution. Opt. Switch. Netw. **6**, 235–242 (2009). https://doi.org/10.1016/j.osn.2009.08.001
Samanta, S., Maity, G.K., Mukhopadhyay, S.: All-optical Walsh-Hadamard code Generation using. In: 2019 Devices for Integrated Circuit (DevIC). pp. 515–518 (2019)
Singh, H., Mittal, N., Miglani, R., Singh, H., Gaba, G.S., Hedabou, M.: Design and analysis of high-speed free space optical (FSO) communication system for supporting fifth generation (5G) data services in diverse geographical locations of India. IEEE Photonics J. **13**, 1–12 (2021). https://doi.org/10.1109/JPHOT.2021.3113650
Wei, Z., Shalaby, H.M.H., Ghafouri-Shiraz, H.: Modified quadratic congruence codes for fiber Bragg-grating-based spectral-amplitude-coding optical CDMA systems. J. Light. Technol. **19**, 1274–1281 (2001)
Xu, Y., Yu, P., Li, Z., Song, Y., Wang, M.: Effect of four-wave mixing on the loss budget of four-channel multiplexing NG-PON systems. J. Mod. Opt. **68**, 37–44 (2021). https://doi.org/10.1080/09500340.2021.1875074
Yeh, C.H., Guo, B.S., Gu, C.S., Chow, C.W., Lin, W.P.: Use of Same WDM Channels in Fiber Network for Bidirectional Free Space Optical Communication with Rayleigh Backscattering Interference Alleviation. IEEE Access. **7**, 169571–169576 (2019). https://doi.org/10.1109/ACCESS.2019.2954951
Yeh, C.H., Chen, J.R., You, W.Y., Chow, C.W.: Hybrid WDM FSO fiber access network with rayleigh backscattering noise mitigation. IEEE Access. **8**, 96449–96454 (2020a)(a). https://doi.org/10.1109/ACCESS.2020.2997820
Yeh, C.H., Xie, Y.R., Luo, C.M., Chow, C.W.: Integration of FSO Traffic in Ring-Topology Bidirectional Fiber Access Network with Fault Protection. IEEE Commun. Lett. 24, 589–592 (2020b). https://doi.org/10.1109/LCOMM.2019.2960221
Yousif, B.B., Elsayed, E.E., Alzalabani, M.M.: Atmospheric turbulence mitigation using spatial mode multiplexing and modified pulse position modulation in hybrid RF/FSO orbital-angular-momentum multiplexed based on MIMO wireless communications system. Opt. Commun. **436**, 197–208 (2019). https://doi.org/10.1016/j.optcom.2018.12.034